A Comparison of Organic and Steam Rankine Cycle Power Systems for Waste Heat Recovery on Large Ships

Andreasen, Jesper Graa; Meroni, Andrea; Haglind, Fredrik

Published in:
Energies

Link to article, DOI:
10.3390/en10040547

Publication date:
2017

Document Version
Publisher's PDF, also known as Version of record

energies

MDPI

Article

A Comparison of Organic and Steam Rankine Cycle Power Systems for Waste Heat Recovery on Large Ships

Jesper Graa Andreasen [1,*], Andrea Meroni [1] and Fredrik Haglind [1]

Department of Mechanical Engineering, Technical University of Denmark, Building 403, Nils Koppels Allé, DK-2800 Kgs. Lyngby, Denmark; andmer@mek.dtu.dk (A.M.); frh@mek.dtu.dk (F.H.)

* Correspondence: jgan@mek.dtu.dk; Tel.: +45-4525-4123

Academic Editor: George Kosmadakis

Received: 15 February 2017; Accepted: 11 April 2017; Published: 17 April 2017

Abstract: This paper presents a comparison of the conventional dual pressure steam Rankine cycle process and the organic Rankine cycle process for marine engine waste heat recovery. The comparison was based on a container vessel, and results are presented for a high-sulfur (3 wt %) and low-sulfur (0.5 wt %) fuel case. The processes were compared based on their off-design performance for diesel engine loads in the range between 25% and 100%. The fluids considered in the organic Rankine cycle process were MM(hexamethyldisiloxane), toluene, n-pentane, i-pentane and c-pentane. The results of the comparison indicate that the net power output of the steam Rankine cycle process is higher at high engine loads, while the performance of the organic Rankine cycle units is higher at lower loads. Preliminary turbine design considerations suggest that higher turbine efficiencies can be obtained for the ORC unit turbines compared to the steam turbines. When the efficiency of the c-pentane turbine was allowed to be 10% points larger than the steam turbine efficiency, the organic Rankine cycle unit reaches higher net power outputs than the steam Rankine cycle unit at all engine loads for the low-sulfur fuel case. The net power production from the waste heat recovery units is generally higher for the low-sulfur fuel case. The steam Rankine cycle unit produces 18% more power at design compared to the high-sulfur fuel case, while the organic Rankine cycle unit using MM produces 33% more power.

Keywords: waste heat recovery; organic Rankine cycle; steam Rankine cycle; off-design; turbine efficiency; diesel engine; marine vessel; container ship; maritime; sustainability; low sulfur fuel

1. Introduction

The majority of goods transported world-wide are carried by sea. Although shipping is environmentally friendly and cost-effective compared to other means of transport, the shipping industry is responsible for large amounts of emissions of CO_2, SO_x (sulfur oxides) and NO_x (nitrogen oxides). Such emissions result from the combustion of fossil fuels like heavy fuel oil (HFO) in the machinery system of the ship.

The machinery systems on marine vessels need to fulfil demands for propulsion power, electrical power and heating. For large vessels, the propeller shaft is coupled directly to a slow speed two-stroke diesel engine, which delivers the required propulsion power. Electricity demands for pumps, fans, lighting, cooling, etc., are typically supplied by four stroke auxiliary engines or alternatively by a shaft generator mounted on the propeller shaft. Heating is required for space heating, HFO preheating and the generation of fresh water. Heating demands can be satisfied by auxiliary oil boilers or from waste heat sources on the ship. For example, heat from the jacket cooling water is typically used in the fresh

water generator, while service steam can be generated in an exhaust gas boiler for satisfying space heating and HFO preheating demands.

In large ships, the heating demands are lower than the available waste heat from the main engine. This enables utilization of the remaining waste heat energy for electricity production by means of suitable waste heat recovery (WHR) technologies. The electricity can either be used on board or for propulsion via a shaft motor mounted on the propeller shaft, thereby replacing the power produced by either the auxiliary engines or the main engine. In this way, the emissions from the machinery system and the fuel consumption can be reduced.

The conventional solution to WHR for electricity production is to employ a power turbine and a dual pressure steam Rankine cycle (SRC) unit. In the case of WHR, the two-stroke diesel engine employs a dedicated tuning where a part of the exhaust gases bypasses the turbochargers. This results in a decrease in mass flow rate through the engine and an increase in the temperature after the turbochargers. The power turbine is installed in the turbocharger exhaust gas bypass for power generation. The SRC unit is installed to utilize the remaining heat in the exhaust gases after the turbocharger and the power turbine for steam evaporation and superheating. Heat from the scavenge air and jacket water is used for preheating.

Hou et al. [1] presented a comparison between the following three conventional WHR options: power turbine unit (stand alone), SRC unit (stand alone) and a combined power turbine and SRC unit. Their investigations suggested that the power turbine stand alone option represents the more economically-feasible option in terms of payback time and return on investment, while the combined solution enables the highest production of electricity. According to MAN Diesel & Turbo [2], the combined power turbine and dual pressure SRC system enables a 11.6% increase of the engine efficiency at full load. The results presented by Ma et al. [3] indicated an engine efficiency increase from 48.5% to 53.8% when installing a single pressure SRC unit in combination with a power turbine unit. Benvenuto et al. [4] suggested an alternative design of the dual pressure SRC unit and demonstrated 34% higher electricity generation at design (SRC stand-alone unit) compared to the dual pressure SRC system design typically used in industry. Dimopoulos et al. [5] showed that the installation of a dual pressure SRC and power turbine-based WHR system is economically feasible with a positive net present value over a wide range of fuel prices and component costs. Theotokatos and Livanos [6] indicated that the use of a single pressure SRC unit for WHR from a dual fuel engine using liquefied natural gas (LNG) enabled lower annual operating costs compared to a diesel-fueled engine with a similar WHR unit. The authors also demonstrated that the use of WHR units enabled a decrease in operating costs.

While the power turbine and SRC solutions are conventionally used for WHR in the marine industry, alternative options like the organic Rankine cycle (ORC) have gained increasing interest. So far, industrial development efforts have been focused on the utilization of heat from the high temperature cooling water loop of marine vessels [7,8]. In the academic field, additional integration options have been investigated for ORC units in many different configurations. Larsen et al. [9] optimized the ORC process for exhaust heat recovery and considered the selection of working fluids taking into account different safety scenarios. The configurations of the ORC process used in this study were both a simple layout and a layout including a recuperator. Yang and Yeh [10,11] considered environmentally-friendly fluids for an ORC unit utilizing heat from the main engine jacket water [10] and ORC units in recuperated and non-recuperated configurations for utilization of exhaust gas heat [11]. Other studies indicated that ORC units in cascade/dual-loop [12–14] and two-stage [15] configurations achieved higher performance than single ORC units for recovery of heat from multiple marine engine waste heat sources [12,15] and for recovery of exhaust gas heat only [13,14].

The studies mentioned above [9–15] considered the design point performance of the WHR units. Although this is a suitable approach for preliminary performance estimations, an off-design analysis must be carried out in order to fully evaluate and compare different WHR unit options by accounting for inherent variations in vessel operation. This point was highlighted by Baldi et al. [16] who

demonstrated the importance of accounting for variations in ship operation, when optimizing a marine machinery system. Larsen et al. [17] studied the NO_x emission and specific fuel oil consumption (SFOC) trade-off for a large marine diesel engine equipped with an ORC bottoming cycle unit while accounting for off-design operation. A combined optimization of the diesel engine, hybrid turbocharger and ORC system yielded NO_x emission reductions of 6.5% and SFOC reductions up to 9%. Ahlgren et al. [18] and Mondejar et al. [19] employed off-design performance estimation methods for evaluating the recovery potential of installing ORC units for exhaust heat recovery on a cruise vessel. The estimated electricity production from the ORC unit corresponded to around 22% of the electricity demand on the cruise vessel.

A few studies have considered a direct comparison between SRC systems and alternative bottoming cycle systems for marine engine WHR. Larsen et al. [20] compared the design point performance of a dual pressure SRC system, an ORC unit and a Kalina cycle power plant. The analysis included performance estimations and qualitative assessments of the three competing WHR technologies. In terms of power production, the ORC unit outperformed the other two, while the SRC unit ranked high in qualitative assessments concerning working fluid safety, environmental properties and familiarity of the technology. Other authors [21–24] compared the off-design performance of single pressure SRC and ORC systems, for recovery of exhaust gas heat only [21,22], for recovery of exhaust gas and scavenge air heat [23] and for recovery of exhaust gas, scavenge air and jacket water heat [24]. These studies all found that the ORC systems achieved higher performance than the single pressure SRC systems. However, to the knowledge of the present authors, there is no previous study comparing the off-design performance of the ORC technology with a state-of-the-art dual pressure SRC power systems (the most advanced/efficient WHR system commercially used today) for utilization of marine engine waste heat. Such a comparison is relevant since previous works have indicated that ORC and SRC systems are the most feasible and promising technologies with respect to WHR on ships. In this context, it is relevant to investigate further under which circumstances each of these systems is preferable. In doing such a comparison, the dual-pressure SRC system is the most relevant reference system because it represents an established and commercially available solution. Additionally, in previous comparisons of WHR systems, the issue of sulfuric acid formation in exhaust gases containing SO_x has not been addressed appropriately. In previous studies, the exhaust gas temperature has been constrained in order to avoid sulfuric acid formation; however, this is insufficient since the coldest spot in the boiler is governed primarily by the boiler feed temperature. Imposing a temperature constraint on the boiler feed temperature has an essential impact on the WHR system layout, since preheating by other sources than the exhaust gases is a requirement for once-through boiler designs, which are typically used in ORC systems.

This paper presents a performance comparison between the well-established dual pressure SRC system and the ORC technology for WHR from the diesel engine on board a 4500 twenty-foot equivalent unit (TEU) container vessel. The comparison is based on simulated off-design performance curves representing the net power output from the WHR systems at various main engine loads. Two cases are considered: one where the sulfur content in the diesel engine fuel is high and one where the sulfur content is low. The two cases employ different constraints for the boiler feed temperature (minimum temperature in the boiler) and service steam demands. The component performance values used in the simulations are selected based on data of a commercial SRC system.

Section 2 presents the adopted methods and outlines the SRC and ORC unit configurations and modeling conditions. Section 3 presents the results of the SRC and ORC unit comparison. Section 4 discusses the results, and Section 5 outlines the conclusions of the study.

2. Methods

2.1. Waste Heat Recovery Systems

Figure 1 shows a sketch of the dual pressure SRC system layout that was analyzed in this study. The pump pressurizes the water from the condenser, which is mixed with the condensed service steam. The water is then preheated by the jacket water in the jacket water cooler. After this, the water flow is directed to the low pressure (LP) and high pressure (HP) steam drums through an additional preheating stage in the scavenge air cooler. At high engine loads, part of the water flow to the LP drum is bypassed the scavenge air cooler in order to control the water inlet temperature to the LP drum. The flows to the steam drums are controlled in order to keep the water levels constant. The second scavenge air cooler bypass line is used at low engine loads, when the scavenge air temperature is lower than the water temperature after the jacket water cooler. A water return line bypassing the steam turbine is illustrated in the sketch, but in all simulations, zero flow was assumed in this line.

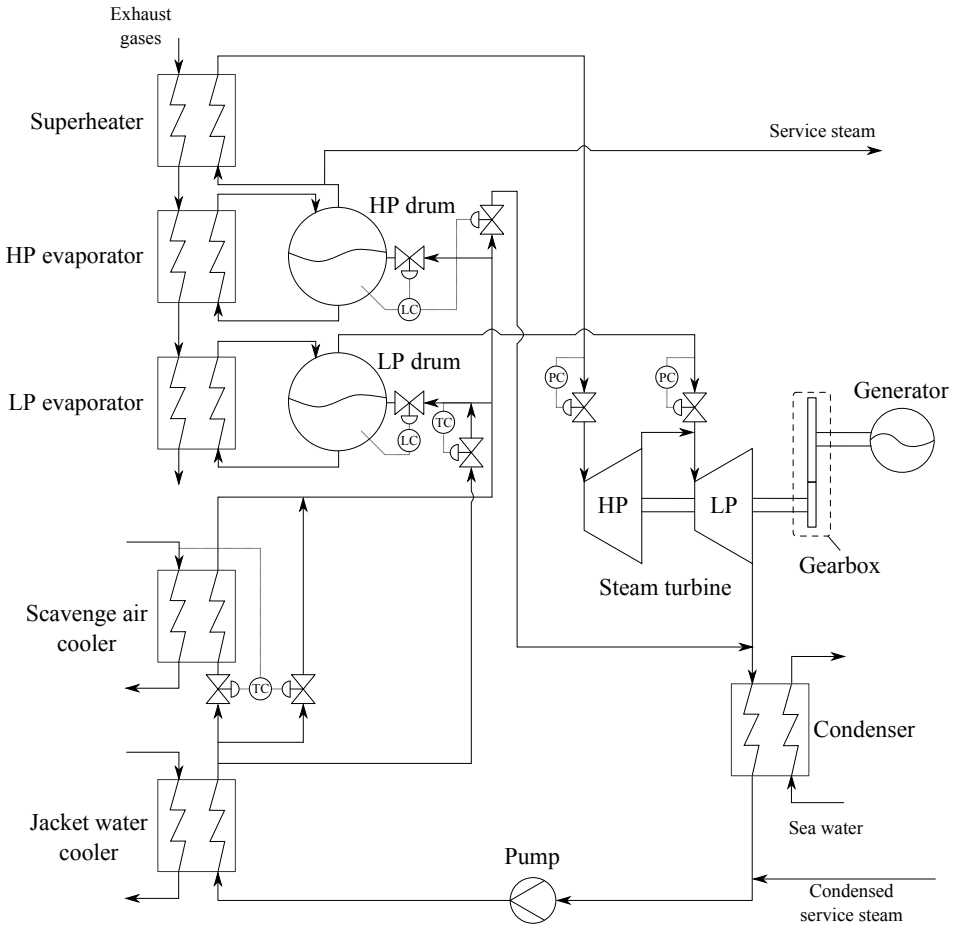

Figure 1. A sketch of the dual pressure steam Rankine cycle (SRC) system with indication of the control purpose of each valve: level control (LC), temperature control (TC) and pressure control (PC).

In the exhaust gas boiler, the water is evaporated in the LP and HP evaporators, and saturated steam is extracted from the top of the LP and HP drums. Part of the saturated HP steam is used as service steam, while the remaining HP steam is superheated and subsequently expanded in the HP turbine. The saturated LP steam is directed from the LP drum to the LP turbine, where it is mixed with the steam from the HP turbine and subsequently expanded in the LP turbine. The two valves at the inlet to the HP and LP turbines control the pressures in the LP and HP parts of the exhaust gas boiler. The HP turbine valve ensures that the HP pressure is always above 7 bar in order to enable a high

enough temperature of the service steam. In conventional systems, the LP turbine valve keeps the LP boiler pressure at a fixed value at 4.5 bar corresponding to a saturation temperature of 148 °C. This control strategy ensures a high enough water temperature at the LP evaporator inlet, which governs the coldest spot in the exhaust gas boiler. If this temperature gets too low, there is a risk of sulfuric acid formation in the exhaust gases resulting in corrosion of tube material in the boiler.

In the final part of the cycle, the steam at the outlet of the steam turbine is condensed in the sea water condenser. The steam turbine is connected to the WHR generator through a reduction gear. Typically, an SRC-based WHR system also includes air ventilation, additional pumps and water tanks between the sea water condenser and the jacket water cooler. These devices ensure the practical operation of the system, but have a limited effect on the thermodynamic performance. Therefore, they were omitted in the analysis of this paper. Following the same rationale, the circulating pumps in the steam drums were omitted.

Figure 2 depicts a sketch of the ORC system. The production of service steam is ensured by placing a service steam boiler in the exhaust gas channel prior to the ORC unit. In the ORC process, the working fluid is pressurized by the pump. Then, it is preheated in the jacket water cooler and subsequently in the recuperator where heat is recovered from the turbine outlet. After the recuperator, the working fluid is preheated, evaporated and superheated in the exhaust gas boiler. The superheated fluid is then expanded in the turbine, where mechanical power is produced. The mechanical power is converted to electricity in the generator. After the turbine, the working fluid is cooled in the recuperator and condensed in a sea water condenser.

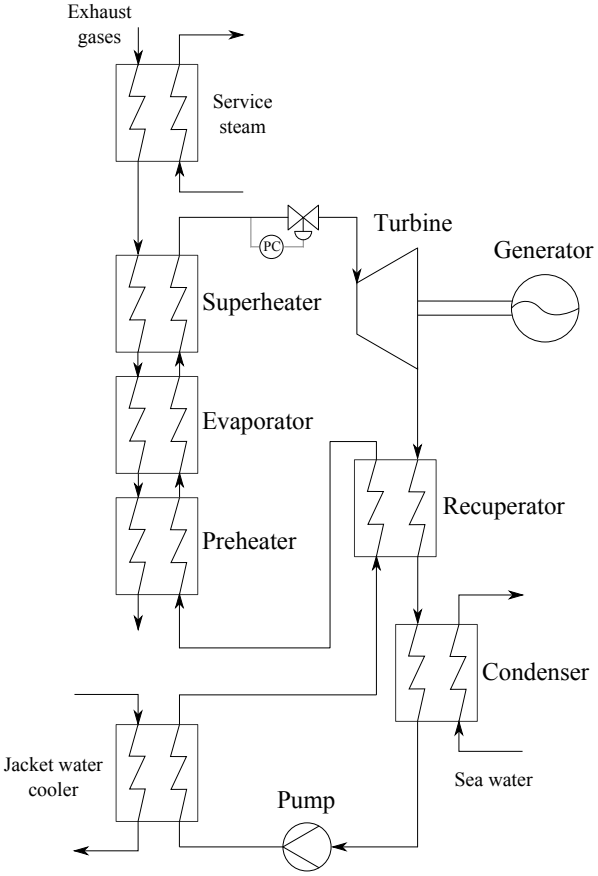

Figure 2. A sketch of the ORC system, with the indication of the control purpose for the turbine inlet valve: pressure control (PC).

As in the SRC system, the boiler feed temperature (preheater inlet, ORC side) must be maintained high enough at all engine loads in order to avoid corrosion of boiler material due to sulfuric acid

formation. This is enabled by controlling the rotational speed of the pump and thereby the working fluid flow rate. The ORC process employs a once-through boiler (no drums) and is thereby relying on preheating prior to the exhaust gas boiler in order to reach the minimum boiler feed temperature. Therefore, the scavenge air heat is not used for preheating, since the temperature decreases significantly at low engine loads. In the ORC process, the recuperator is used for preheating instead of the scavenge air cooler, since it enables preheating to a high temperature even at low engine loads. A requirement for this is that the working fluid temperature at the outlet of the turbine is high, i.e., the working fluid must be a sufficiently dry fluid. The pressure control valve at the turbine inlet is included in order to ensure that the pressure before the valve does not decrease to a point where evaporation occurs in the recuperator. In the SRC process, the decreasing scavenge air temperature is not an issue in relation to sulfuric acid formation, because the constant LP pressure control ensures a constantly high LP evaporator feed temperature. The use of scavenge air heat for feed water preheating has a beneficial impact on the performance of the system and is therefore typically employed in SRC processes.

The working fluids considered in the ORC unit were selected among fluids commonly employed by ORC suppliers at heat source temperatures above 200 °C. For a heat source temperature above 200 °C, such fluids are n-pentane, MDM, solkatherm, toluene, R245faand R134a [25]. The following fluids were included since they are molecularly similar to n-pentane and MDM: i-pentane, c-pentane and MM. Fluids that are subjected to a gradual phase-out (R245fa and R134a) [26,27], and fluids with decomposition temperature below 300 °C (solkatherm) [28,29] were excluded from the list of considered fluids. Fluids with condensation pressures lower than that of water at 35 °C (MDM) were also excluded, in order to avoid issues with high rates of air infiltration. The final list of fluids considered in this study was thereby: MM, toluene, n-pentane, i-pentane and c-pentane.

2.2. Marine Vessel and Main Engine Characteristics

The comparison is based on a Maersk Line container vessel, which is equipped with a 23-MW two-stroke MAN diesel engine and a WHR system comprising a power turbine and a dual pressure SRC unit. According to the recommendations by MAN Diesel & Turbo [2], SRC and/or power turbine systems are relevant for engine sizes larger than 15 MW, while ORC or power turbine systems are relevant for smaller engine and WHR system sizes. With a 23-MW engine, the container vessel is near the lower feasibility limit for a dual pressure SRC unit installation. At low power outputs, the ORC technology is typically more advantageous compared to the SRC technology [2,25,30]. The vessel does therefore represent a relevant case for making a comparison between the SRC and ORC systems.

The diesel engine data used in the performance estimations of the WHR systems were the exhaust gas temperature, scavenge air temperature, air mass flow rate and jacket water cooling heat rate. The exhaust gas temperature is defined as the temperature after mixing of the turbocharger and power turbine exhaust gas streams, and the scavenge air temperature is defined as the air temperature after the turbocharger compressor. The exhaust gas temperature, scavenge air temperature and air mass flow rate were based on measured values from the actual engine installed on the container vessel, while the jacket water heat amount was computed from the online CEAS engine calculation tool provided by MAN Diesel & Turbo [31]. Figure 3 depicts the variation of the four engine parameters mentioned above. The markers represent data points that were available from measurements or CEAS data. The values were interpolated for the remaining engine loads.

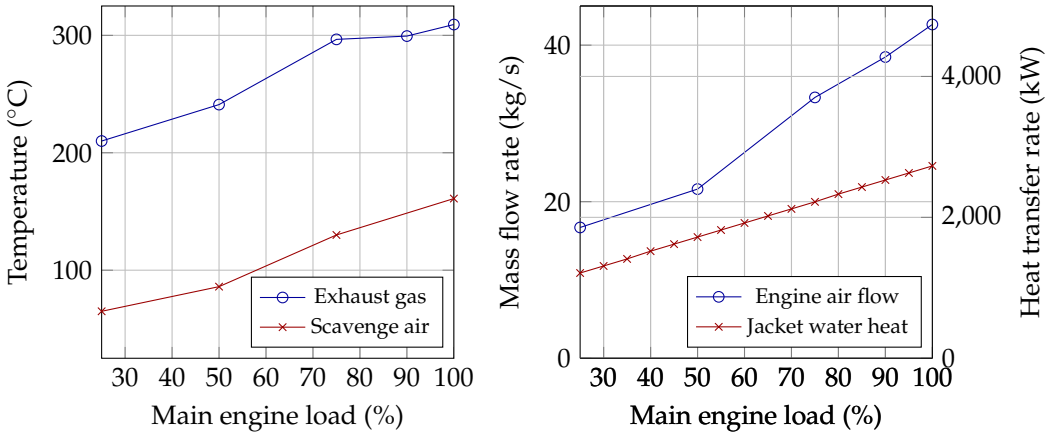

Figure 3. Selected characteristics of the MAN 6S80ME-C9 engine installed on the container vessel. (**a**) Temperatures; (**b**) mass and heat flow.

2.3. Numerical Simulations

The heat inputs to the SRC and ORC units were delivered from the exhaust gases, scavenge air and jacket water, while heat was rejected to the sea water. Constant values of specific heat capacity were assumed for the exhaust gases and scavenge air, and the jacket water and sea water were modeled using the properties of water. The thermodynamic properties of water and the organic fluids were computed using the open source software Coolprop [32].

The simulations included two different cases: one where the diesel engine used a high-sulfur fuel and one where it used a low-sulfur fuel. The high-sulfur fuel case represents combustion of HFO with a weight-based sulfur content of 3%, while the low-sulfur fuel case represents combustion of a fuel containing 0.5% sulfur (by weight) in compliance with the upcoming regulation imposed by the International Maritime Organization (IMO) [33]. In the case of high-sulfur fuel, the boiler feed temperature was constrained to a minimum value of 148 °C. This corresponded to the situation encountered in existing ships with SRC-based WHR systems [2]. In the low-sulfur fuel case, the minimum boiler feed temperature was set to 125 °C, which is slightly higher than the acid dew point temperature at 0.5 wt % fuel sulfur content approximated by MAN Diesel & Turbo [34]. The low-sulfur fuel case represents an engine using marine diesel oil (MDO) or marine gas oil (MGO) with low sulfur contents or a dual fuel engine using LNG and HFO as a pilot fuel.

2.3.1. Design Models

Table 1 provides an overview of the general modeling conditions. The performance values for the turbine and heat exchangers were selected based on the SRC model validation; see Section 2.3.3. The WHR systems were designed at 100% main engine load, while the highest load point included in the validation was 90%. Since both the isentropic efficiency of the turbine and the pinch points of the heat exchangers tend to decrease as a function of the WHR unit load, the values selected in Table 1 were slightly higher than those extracted from the measured data. The turbine design efficiencies were linearly extrapolated from 90% to 100% engine load. The pinch points of evaporators and superheaters were given a value of 20 °C at design, since it results in a good trade-off between minimizing the risk of soot formation and maximizing steam production [34].

Table 1. General modeling conditions.

Parameter	Value	Process
Fixed parameters		
Exhaust gas heat capacity [kJ/(kg K)]	1.06	SRC & ORC
Scavenge air heat capacity [kJ/(kg K)]	1.02	SRC
Temperature after jacket water preheater [°C]	80	SRC & ORC
Jacket water heat used in fresh water generator [kW]	400	SRC & ORC
Condensation temperature [°C]	35	SRC & ORC
Isentropic efficiency of HP/ORC turbine [%]	62	SRC & ORC
Isentropic efficiency of LP turbine [%]	62	SRC
Isentropic efficiency of pump [%]	70	SRC & ORC
Generator efficiency [%]	93	SRC & ORC
Relative pressure drop in heat exchangers [%]	3	SRC & ORC
Approach temperature difference HP drum [°C]	10	SRC
Approach temperature difference LP drum [°C]	8	SRC
Isentropic efficiency of sea water pump [%]	70	SRC & ORC
Sea water heat capacity [kJ/(kg K)]	4	SRC & ORC
Pressure rise across sea water pump [bar]	2	SRC & ORC
Temperature difference of sea water in condenser [°C]	5	SRC & ORC
Sea water density [kg/m^3]	1000	SRC & ORC
Minimum temperature difference in recuperator [°C]	20	ORC
Constraints		
Minimum temperature difference superheater [°C]	20	SRC & ORC
Minimum temperature difference HP/ORC evaporator [°C]	20	SRC & ORC
Minimum temperature difference LP evaporator [°C]	20	SRC
Minimum vapour quality at turbine outlet [-]	0.88	SRC & ORC

Table 2 lists the modeling conditions and the ranges for the decision variables (optimized variables), which were specific for each case. The four cases comprised a high-sulfur and a low-sulfur fuel case for each of the SRC and ORC processes. For the high-sulfur case, the boiler feed temperature was high due to the high SO_x contents in the exhaust gases. The service steam rates for the high-sulfur fuel case were based on the SRC unit design values for the container vessel. The steam is used for HFO tank heating, HFO preheating prior to engine injection and space heating on the ship. The use of low-sulfur fuel implies no or limited use of HFO. It was therefore assumed that the service steam demands were halved for the low-sulfur fuel case compared to the high-sulfur fuel case, leaving service steam for space heating and possibly pilot fuel heating for dual fuel engines.

Table 2. Case specific modeling conditions for high-sulfur (HS) and low-sulfur (LS) fuels.

Parameter	SRC, HS-Fuel	ORC, HS-Fuel	SRC, LS-Fuel	ORC, LS-Fuel
Decision variables				
HP/ORC boiler pressure (bar)	7–20	1–0.8·P_{crit}	7–20	1–0.8·P_{crit}
LP boiler pressure (bar)	4.5–7	-	1–7	-
Pressure drop across LP turbine valve (bar)	0–5	-	0–5	-
Degree of superheating (°C)	5–50	5–50	5–50	5–50
HP/ORC turbine mass flow rate (kg/s)	0.5–5	2–40	0.5–5	2–40
LP turbine mass flow rate (kg/s)	0.1–5	-	0.1–5	-
Constraints				
Minimum boiler feed temperature (°C)	148	148	125	125
Service steam demand				
Service steam mass flow rate (kg/h)	1730	1730	865	865

The WHR systems were optimized by maximizing the net power output. The design point net power output was calculated as:

$$\dot{W}_{net,0} = \eta_{g,0} \cdot \dot{W}_{t,0} - \dot{W}_{wf,p,0} - \dot{W}_{sw,p,0} \quad (1)$$

where $\eta_{g,0}$ is the design efficiency of the generator, $\dot{W}_{t,0}$ is the design mechanical power generated by the turbine, $\dot{W}_{wf,p,0}$ is the design power consumption of the working fluid pump and $\dot{W}_{sw,p,0}$ is the design power consumption of the sea water pump. For the SRC process, $\dot{W}_{t,0}$ is the sum of the mechanical power generated in the HP and LP turbines.

2.3.2. Off-Design Models

Typically, WHR units on ships are operated in off-design due to the operation of the main engine at various load points and ambient conditions. In the numerical simulations carried out in this paper, the performance of the WHR-systems were changing due to variations in the exhaust gas and scavenge air flows and temperatures with engine load; see Figure 3.

The performance of heat exchangers, turbines and pumps is affected by changes in operating conditions. The performance variation of the heat exchangers, where one fluid was a gas or vapor, were modeled based on variations in the overall UAvalue (product of the overall heat transfer coefficient, U, and the heat transfer area, A) of the heat exchangers. In these heat exchangers, the gas or vapor side was assumed to dominate the heat transfer processes resulting in a UA value variation governed by the gas or vapor mass flow rate. The UA value at any off-design point was assumed to vary according to the following function, which is commonly used for simulating off-design characteristics of heat exchangers in power cycles [16,18,19,35]:

$$\frac{UA}{UA_0} = \left(\frac{\dot{m}}{\dot{m}_0}\right)^{\gamma} \quad (2)$$

where subscript 0 refers to the design point value of UA and gas/vapor mass flow rate $\dot{m}$ and γ is an exponent describing the relationship between mass flow rate and heat transfer coefficient of the gas/vapor.

Equation (2) was applied for modeling the off-design performance of the following heat exchangers: scavenge air cooler ($\gamma = 0.6$), recuperator ($\gamma = 0.6$), LP evaporator ($\gamma = 0.6$), HP evaporator ($\gamma = 0.6$), preheater ($\gamma = 0.6$), evaporator ($\gamma = 0.6$) and superheater ($\gamma = 0.8$). The values of γ were selected based on the mass flow rate exponent appearing in the heat transfer correlations. A value of $\gamma = 0.6$ was assumed for flow outside tubes [36,37], and $\gamma = 0.8$ was assumed for in-tube flow [38]. In the superheater, the mass flow rate in Equation (2) was assumed to be that of the working fluid. The jacket water coolers and the condensers were not modeled according to Equation (2). It was assumed that the jacket water cooler preheated the fluid to 80 °C at all loads. Moreover, it was checked that the heat transfer in the jacket water cooler did not exceed the heat available from the engine at the given load point. The condensation temperature was assumed to remain constant at all loads.

The pressure drops in the systems were assumed to vary according to the following expression [39]:

$$\frac{\Delta P}{\Delta P_0} = \left(\frac{\dot{m}}{\dot{m}_0}\right)^2 \quad (3)$$

A constant value of pressure drop was assumed in the sea water system independently of the main engine load.

The variation of the working fluid pump efficiency was estimated according to the following polynomial expression extracted from Veres [40]:

$$\frac{\eta_p}{\eta_{p,0}} = -0.029265\left(\frac{\dot{V}}{\dot{V}_0}\right)^3 - 0.14086\left(\frac{\dot{V}}{\dot{V}_0}\right)^2 + 0.3096\left(\frac{\dot{V}}{\dot{V}_0}\right) + 0.86387 \quad (4)$$

where $\dot{V}$ is the volume flow rate at the pump inlet and $\eta_{p,0}$ is the pump design efficiency. Compared to the original expression presented by Veres [40], the change of pump efficiency with rotational speed was neglected. It was assumed that the efficiency of the sea water pump was equal to the design value at all off-design conditions.

The isentropic efficiencies of the turbines were assumed to vary according to the following function:

$$\frac{\eta_t}{\eta_{t,0}} = 0.4097 \left(\frac{\dot{m}_{wf}}{\dot{m}_{wf,0}} \right) + 0.5903 \tag{5}$$

where $\dot{m}_{wf}$ is the working fluid mass flow rate and $\eta_{t,0}$ is the turbine design efficiency. The function was generated by fitting the experimental data presented by Erhart et al. [41] for an ORC unit using MDM as the working fluid. This function was selected since it resulted in accurate turbine power estimations in the SRC model validation; see Section 2.3.3. For the turbines, the Stodola constant was used to express the relationship between mass flow rate, inlet and outlet pressures and inlet temperature [42]:

$$C_T = \frac{\dot{m}\sqrt{T_{in}}}{\sqrt{{P_{in}}^2 - {P_{out}}^2}} \tag{6}$$

where T_{in} is the turbine inlet temperature, $\dot{m}$ is the mass flow rate through the turbine and P_{in} and P_{out} are the turbine inlet and outlet pressures. In the SRC model, the turbine constant was calculated for the HP and LP turbine separately.

The generator efficiency was assumed to vary according to the following expression [43]:

$$\eta_g = \frac{\eta_{g,0} \left(\frac{\dot{W}_t}{\dot{W}_{t,0}} \right)}{\eta_{g,0} \left(\frac{\dot{W}_t}{\dot{W}_{t,0}} \right) + (1 - \eta_{g,0}) \left[(1 - F_{CU}) + F_{CU} \left(\frac{\dot{W}_t}{\dot{W}_{t,0}} \right)^2 \right]} \tag{7}$$

where F_{CU} is the copper loss fraction, which is assumed to have a value of 0.43, and $\eta_{g,0}$ is the generator design efficiency.

2.3.3. SRC Model Validation

The model of the SRC system was validated by comparing the model outputs with measured data from the dual pressure SRC system on a Maersk Line container vessel. The data were measured during the sea trials. The data contain measurements from three different days collected during a time period of 10–15 min. The values used in the validation were averaged over these time intervals for each of the three days. All three datasets contain measurements at 90%, 75% and 50% main engine load, while Dataset 1 contains an additional measurement at 40% main engine load. The measured data (proprietary information of Maersk), which were used in the validation, are listed in Table 3.

The first step in the validation was to select the 90% main engine load point in Dataset 1 as the design point for the SRC unit. This data point was then used in the design model to define the design of the SRC unit. Values for the temperature of the exhaust gases and scavenge air were used directly from the dataset along with HP and LP boiler pressures and mass flow rates and the intermediate pressure (IP) between the HP and LP turbines. The exhaust gas mass flow rate was calculated based on flow characteristic curves for the turbochargers and power turbine. The scavenge air mass flow rate was assumed to be equal to that of the exhaust gases, neglecting the mass flow rate of fuel, which is <5% of the exhaust gas mass flow rate. The approach temperature difference of the HP and LP drums was extracted based on the measured drum feed temperatures and pressures. Similarly, the degree of superheating was extracted from the measured HP steam (HP turbine inlet) temperature and pressure. It was assumed that the HP and LP turbines have the same isentropic efficiency. The isentropic efficiency of the turbines were tuned in order to match the estimated steam turbine generator output ($\eta_g \cdot \dot{W}_t$) with the measured value. In the validation, the constraints listed in Table 1 were not employed.

The input parameters to the design model, which were not mentioned in the above, were given the assumed values listed in Table 1, and the service steam production was assumed to be zero. The design model was then used to estimate the power output at 90% engine load for Dataset 1 and to calculate the design point parameters used in Equations (2)–(7). For the remaining measured engine load points, the off-design model was used to estimate the variations in steam turbine generator output, steam pressures, steam mass flow rates and steam temperatures.

Figure 4 shows the comparison of the SRC model output and the measured values, and Table 3 lists the details on the location of mass flow rate, pressure and temperature measurements. In Figure 4a are compared estimated and measured values of the electric power generated in the steam turbine generator for Dataset 1. An exact match between the model and the measured data was obtained at 90% main engine load, since this point was selected as the design point for the SRC model validation. At 75%, 50% and 40% main engine load, the model estimations were within 2.3%, 2.4% and 11.9% of the measured values, respectively. The larger deviation at 40% main engine load could be due to the zero flow of LP steam to the turbine at this load point, which might result in inaccuracies in the turbine efficiency function in Equation (5). The maximum relative deviations for the HP and LP mass flow rates (see Figure 4b) were below 4% and 15%, respectively. The relative deviations for the pressure predictions in Figure 4c were below 2% for the HP pressure and below 22% for the IP pressure, while the relative deviations for the temperature predictions displayed in Figure 4d were below 2%.

The comparison with the measurements in Dataset 2 indicates that the model overestimates the power (see Figure 4e) and HP mass flow rate (see Figure 4f) up to 14.3% and 51.2%, respectively. Note that the high percentage value for the HP mass flow rate prediction was due to the values being relatively small at 50% main engine load. The overestimation of HP pressure was up to 8.2%; see Figure 4g. Accurate estimations were achieved for the LP steam flow (maximum difference: 0.21 kg/s), the pressure between the HP and LP turbines (maximum difference: 0.12 bar) and the temperatures (maximum difference: 6.2 °C). This indicated that the assumption of zero service steam production might not be correct for Dataset 2. By taking out saturated service steam from the HP steam drum, the mass flow rate to the HP turbine would drop. As a consequence, the HP steam pressure would drop according to the Stodola constant calculated for the HP turbine; see Equation (6). The drops in HP steam flow and pressure would result in a drop in the SRC turbine power production, thus resulting in a better match between the estimated and measured values. The relative deviations of the temperature predictions in Figure 4h were below 3%.

For Dataset 3, the electrical power generation was estimated with discrepancies of 1.0%, 3.1% and 9.8% at main engine loads of 90%, 75% and 50%, respectively; see Figure 4i. The deviations for the HP and LP mass flow rates in Figure 4j were below 4% and 18%, respectively. The HP and IP pressure predictions (Figure 4k) were within 7% and 10% of the measured values, respectively, while the temperature predictions (Figure 4l) were within 4%.

Table 3. Relevant data available in the datasets.

Main engine power
Steam turbine generator output
HP steam pressure
HP steam temperature before HP turbine valve
HP steam flow to HP turbine
LP steam pressure
LP steam temperature after LP turbine valve
LP steam flow to LP turbine
Intermediate pressure between LP and HP turbines (IP)
Condenser pressure
HP feed water temperature at HP drum inlet
LP feed water temperature at LP drum inlet
Exhaust gas temperature

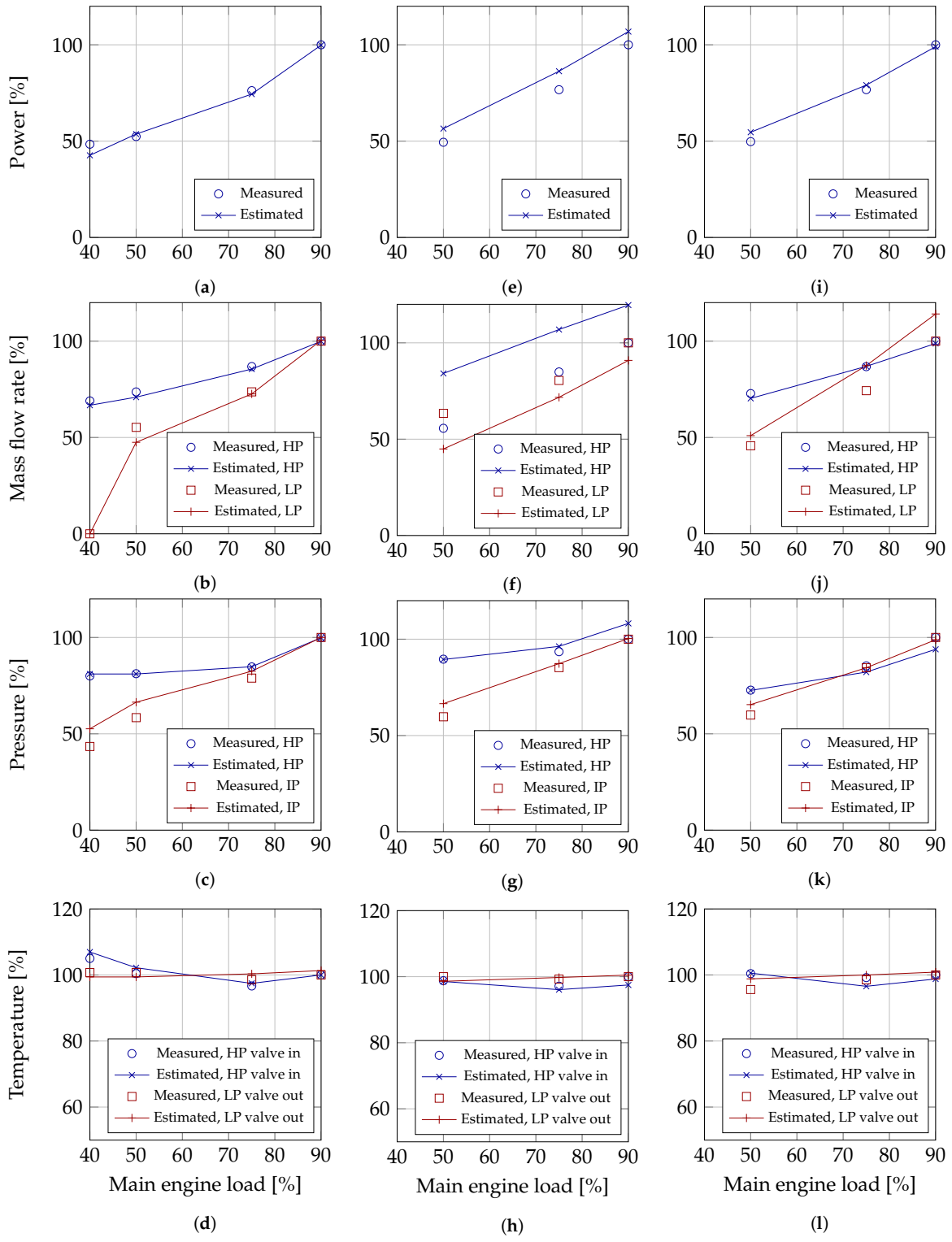

Figure 4. SRC model validation with three datasets (DS); values normalized with measured value at 90% main engine load. (**a**) DS 1, power; (**b**) DS 1, flow; (**c**) DS 1, pressure; (**d**) DS 1, temperature; (**e**) DS 2, power; (**f**) DS 2, flow; (**g**) DS 2, pressure; (**h**) DS 2, temperature; (**i**) DS 3, power; (**j**) DS 3, flow; (**k**) DS 3, pressure; (**l**) DS 3, temperature

Based on the comparison with experimental data and the discussions above, the model was considered valid and suitable for the comparisons carried out in this paper.

3. Results

In this section, the results of the simulations are presented. First, the design and off-design performance characteristics of the SRC and ORC processes are compared for the high and low-sulfur fuel cases. Subsequently, the comparison is carried out for different values of the turbine design efficiency.

3.1. High-Sulfur Fuel Engine

The WHR system designs resulting from the design optimizations are listed in Table 4 for the high-sulfur fuel case. The only feasible fluids resulting from the optimizations are water (SRC) and MM (ORC). The remaining working fluids are not able to reach boiler feed temperatures of 148 °C, since the heat available for preheating in the recuperator is not enough. For the SRC process, the preheating with scavenge air and jacket water enables a sufficiently high boiler feed temperature. MM is a very dry fluid and is therefore, as the only organic working fluid, able to preheat the working fluid sufficiently in the recuperator.

Table 4. Waste heat recovery (WHR) unit design results for the high-sulfur fuel case.

Fluid	$\dot{W}_{net}$ (kW)	$P_{HP/ORC}$ (bar)	P_{LP} (bar)	P_{IP} (bar)	P_{cond} (bar)	T_{sup} (°C)	$\dot{m}_{HP/ORC}$ (kg/s)	$\dot{m}_{LP}$ (kg/s)	ρ_{ratio} (-)	UA_{total} (kW/K)
Water	981	15.1	4.5	4.5	0.056	50	1.31	1.07	149	163
MM	821	8.8	–	–	0.090	28	15.7	–	106	234

The SRC process achieves a net power output at design 19% larger than the ORC process using MM as the working fluid. The pressures in the two cycles have similar orders of magnitude with sub-atmospheric pressures in the condensers. The overall density ratio across the turbine (ρ_{ratio}) is 41% higher for the SRC (calculated between HP turbine inlet and LP turbine outlet) than the ORC process. The higher values of density ratio and mass flow rates across the ORC turbine suggest higher values of turbine efficiency and a simplified design with a lower number of stages. The total UA value (UA_{total}) for the ORC process comprises the preheater, evaporator, superheater and recuperator UA values, while it includes the scavenge air cooler, LP and HP evaporators and superheater for the SRC unit. Although the heat transfer coefficient varies for the different heat exchangers, the total UA values were used as a basis for comparing the heat transfer area requirement for the different WHR processes. The total UA value is 44% larger for the ORC unit and suggests that larger heat transfer equipment is required compared to the SRC unit.

Figure 5a depicts the off-design behavior for the SRC and ORC processes for the high-sulfur fuel case. The sudden slope changes at 75% main engine load are a result of the exhaust gas temperature variation; see Figure 3a. As the main engine load drops, the performance difference between the SRC and the ORC processes decreases, and at engine loads between 65% and 55%, the ORC unit produces slightly more power than the SRC unit. The power output from the SRC unit drops faster than the ORC unit power, due to higher throttling losses. The LP turbine valve throttles the LP steam already from 95% main engine load in order to maintain the pressure in the LP drum, which is required due to the boiler feed temperature limitation. The HP turbine and the ORC turbine valves are both active for main engine loads below 60%.

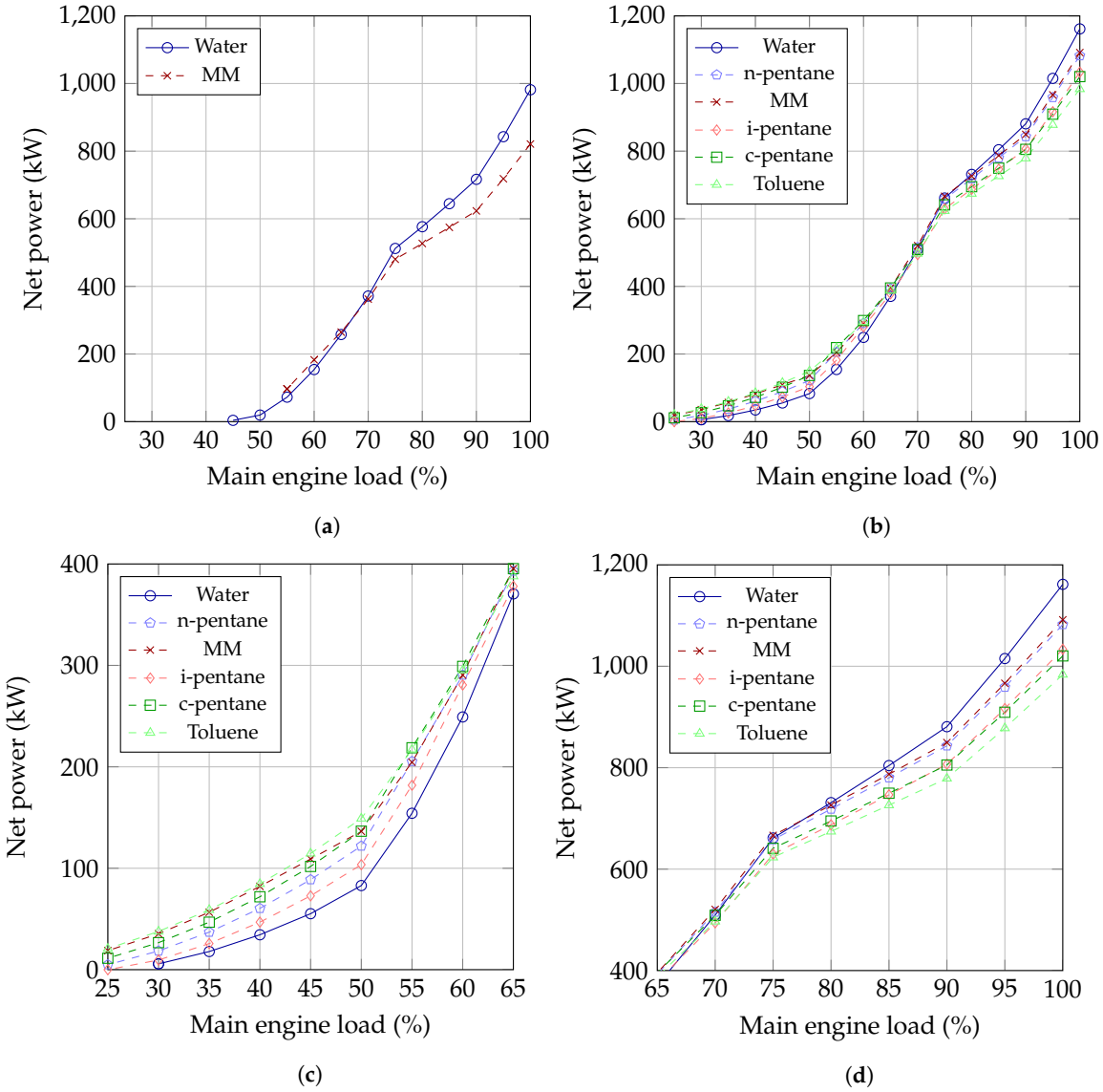

Figure 5. Off-design curves. (**a**) High-sulfur fuel; (**b**) low-sulfur fuel; (**c**) low-sulfur fuel, low load; (**d**) low-sulfur fuel, high load.

3.2. Low-Sulfur Fuel Engine

Table 5 lists the WHR system solutions resulting from the design optimizations for the low-sulfur fuel case. The WHR units reaching the highest net power outputs are the SRC unit and the ORC units with MM and n-pentane as the working fluid. Compared to the high-sulfur fuel case, higher net power outputs are reached due to the lower service steam demands and less strict requirements for the minimum boiler feed temperature. The lower minimum boiler feed temperature enables a reduction in the LP drum pressure from 4.5 down to 2.3 bar, corresponding to a temperature drop from 148 down to 125 °C, which is beneficial for the performance of the SRC unit. For the SRC unit, the design power is 18% higher for the low-sulfur fuel case compared to the high-sulfur fuel case, while it is 33% higher for the ORC unit using MM as the working fluid. In terms of net power output, MM and n-pentane are followed by i-pentane and c-pentane, which reach slightly lower net power outputs. Toluene achieves the lowest net power output. The pressure levels are highest in the ORC unit using n-pentane and i-pentane. The high boiler pressure is a drawback, while it is beneficial that the condenser pressure is above or close to atmospheric pressure. The working fluid mass flow rates in all of the ORC units are

significantly higher than in the SRC unit. The density ratio across the turbine is below 35 for n-pentane, i-pentane and c-pentane, indicating that efficient axial turbines using few stages can be designed for these fluids. Among the ORC units, the c-pentane and toluene solutions require the lowest UA values, with values that are, respectively, 11% higher and 6% lower than those of the SRC unit. The total UA value of the ORC unit using MM is 73% higher than the total UA value of the SRC unit.

Table 5. WHR unit design results for the low-sulfur fuel case.

Fluid	$\dot{W}_{net}$ (kW)	$P_{HP/ORC}$ (bar)	P_{LP} (bar)	P_{IP} (bar)	P_{cond} (bar)	T_{sup} (°C)	$\dot{m}_{HP/ORC}$ (kg/s)	$\dot{m}_{LP}$ (kg/s)	ρ_{ratio} (-)	UA_{total} (kW/K)
Water	1162	11.8	2.3	2.3	0.056	47	1.78	1.27	120	174
MM	1091	9.45	–	–	0.090	5	22.1	–	125	302
n-pentane	1082	27.0	–	–	0.98	38	14.8	–	31	281
i-pentane	1034	27.0	–	–	1.29	43	15.6	–	23	262
c-pentane	1020	19.2	–	–	0.62	49	12.0	–	31	194
Toluene	984	4.69	–	–	0.062	50	11.1	–	67	163

The off-design performance curves for the low-sulfur fuel case are shown in Figure 5b. Figure 5c,d shows the same curves, but zooms in on the low and high main engine loads respectively. As for the high-sulfur fuel case, the performance of the SRC unit drops faster than that of the ORC units when the main engine load decreases. At 65% load and below, the SRC unit performance is lower than all of the ORC units. The fluids i-pentane and c-pentane achieve similar net power outputs at design conditions, but c-pentane is performing better at low main engine loads. At low loads, MM, toluene and c-pentane reach the highest net power outputs among the considered fluids.

3.3. Turbine Efficiency Variation

As indicated in the fluid comparison for the high and low-sulfur fuel cases, the attainable isentropic efficiency for a given turbine investment cost might be different depending on the properties of the fluids. Steam turbines are typically difficult to design with high efficiencies for low power applications, due to high specific enthalpy and volume/density changes during the expansion [44] combined with low mass flow rates and liquid formation in the last part of the turbine. These issues are generally less pronounced or even non-existing for organic fluids, which can enable high efficiency organic turbines with simple designs using few turbine stages (see the detailed discussion in Section 4.1). The process design optimizations and off-design calculations were therefore repeated to illustrate the impact of the turbine design efficiency on the net power output.

For the high-sulfur fuel case, the SRC unit and the ORC unit using MM were compared, and for the low-sulfur fuel case, the SRC unit and the ORC unit using c-pentane were compared. The reason for selecting c-pentane is that it enables high net power output at high and low loads, with low values for the density ratio and total UA value.

Figure 6a illustrates the impact of the design isentropic turbine efficiency on the SRC and ORC unit off-design performance curves for the high-sulfur fuel case. The design point performance of the SRC unit has a large increase when the turbine efficiency is increased from 62–72%, but the increase from 72–82% does not result in a corresponding net power increase. This is because the higher turbine efficiency makes it necessary to throttle the LP steam before the turbine in order to avoid more than 12% liquid water at the LP turbine outlet. The throttling of the LP steam also has a negative effect on the performance at low engine loads, where the $\eta_{t,0} = 82\%$ solution performs worse than the solutions with lower turbine efficiency. Equivalent to the results presented in Figure 5, the ORC units are able to maintain higher net power outputs at low loads. In case the MM turbine is 10% points more efficient than the steam turbine, e.g., $\eta_{t,0} = 72$ % versus $\eta_{t,0} = 62\%$, the net power of the ORC unit is larger than the SRC unit up to 90% engine load; see Figure 6a. In case the design efficiency of the MM turbine

is $\eta_{t,0} = 82\%$ and the steam turbine efficiency is $\eta_{t,0} = 72\%$, then the ORC unit net power output surpasses the SRC unit up to 80% engine load.

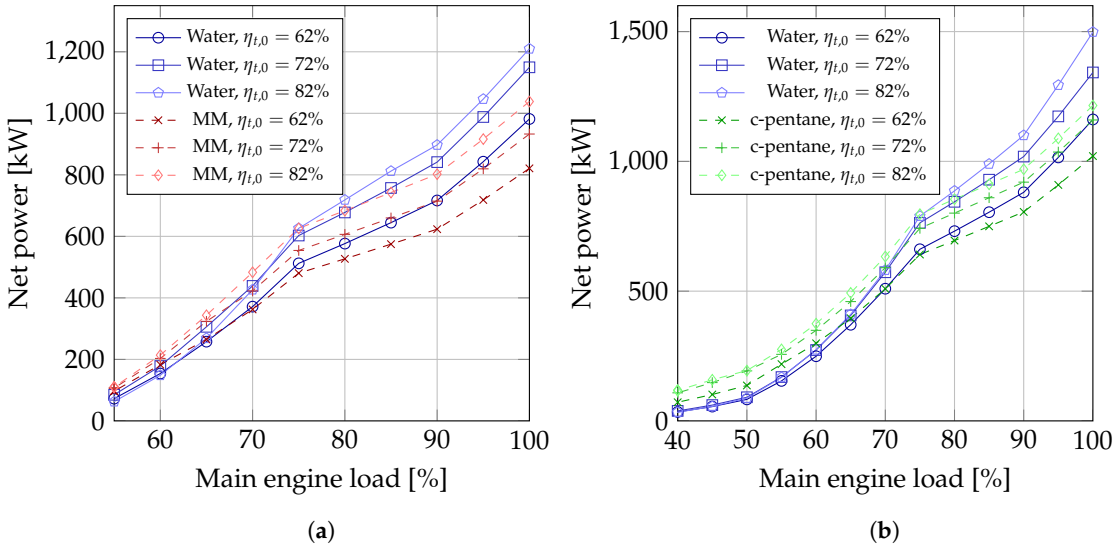

Figure 6. Off-design curves for different turbine efficiencies. (**a**) High-sulphur fuel; (**b**) Low-sulphur fuel.

Figure 6b shows the effect of varying the turbine efficiency for the low-sulfur fuel case. The comparison was made between the SRC unit and the ORC unit using c-pentane. Considering a 10% point turbine efficiency difference with $\eta_{t,0} = 72\%$ for the c-pentane turbine and $\eta_{t,0} = 62\%$ for the steam turbine, the ORC unit net power output is the largest for all engine loads. With $\eta_{t,0} = 82\%$ for the c-pentane turbine and $\eta_{t,0} = 72\%$ for the steam turbine, the net power output of the ORC unit is the largest up to 80% engine load. For the low-sulfur fuel case, the ORC unit performance is significantly higher than the SRC unit for engine loads below 50%.

4. Discussion

4.1. Turbine Design and Efficiency

The design of high-efficiency axial turbines for low power outputs becomes inherently limited using steam as the working fluid. Macchi [45] and Owen [46] argued that single-stage solutions with steam are impractical since they would require high supersonic flows in the blade row, high peripheral speed, high liquid content at turbine discharge and high volumetric ratios between outlet and inlet. If a limited number of stages is selected, the large enthalpy drop (>500 kJ/kg) yields high nozzle efflux velocities, with issues related to the high rotational speed and Mach numbers in the stages. The small mass flow rate required at low power outputs would result in small flow passages, increasing friction and clearance losses. Moreover, disc friction and windage losses would be large, and partial admission is required in the first stages, increasing losses and complexity. The overall result would be a low turbine efficiency. A high number of stages is then required to achieve acceptable values of efficiency, making the solution complex and economically unattractive [47].

The turbine efficiency value of 62% used in the initial comparison of the SRC and ORC units (Figure 5 and Tables 4 and 5) was based on the SRC model validation with measured data. Table 6 lists the design efficiency of some documented steam and organic turbines in the low power output range. The table shows that commercial steam turbine units achieve values between 52% and 71% for power capacities in the range 500–1000 kW, according to number of stages and turbine configuration. The efficiency values fall down to 50% for power capacities around 500 kW. Similar values are obtained

for very small steam turbines using advanced designs [48]. These considerations indicate that the initial assumption of 62% is representative for state-of-the-art steam turbines for marine applications.

Table 6. Design efficiency and power output of some documented axial turbines for SRC and ORC.

Author	Ref.	Year	Fluid	$\eta_{t,0}$ (%)	Power (kW)	Stages
Angelino et al.	[47]	1983	water	60	1000	1
Verdonk and Dufournet	[49]	1987	water	64.9	1356	1
Bahadori and Vuthaluru	[50]	2010	water	52–71	1000	multistage
				55–66	500	multistage
Darrow et al.	[51]	2015	water	52.5	500	multistage
				61.2	3000	multistage
Elliot	[52]	2016	water	60–67 (*)	<10,000	multistage
Kraus et al.	[48]	2016	water	50–53.2	26.4–42.5	2
Angelino et al.	[47]	1983	organic	82.8 (*)	1000	2
Angelino et al.	[53]	1993	organic	83.1	1300	1
Verneau	[54]	1987	Fluorinol	80	1300	2
			FC-75	78	50	2
			FC-75	75	50	1
Klonowicz et al.	[55]	2014	R227ea	54	10	1

(*) = Value estimated by the numerical prediction method.

It is arguable that higher efficiencies, up to 85%, can be achieved with organic fluids for the power range investigated in this study. Due to the large molecular mass of organic fluids, the small values of enthalpy drop (typically between 10 and 100 kJ/kg) permit the use of turbine units with reduced number of stages, rotational speed and centrifugal stresses. Concurrently, the presence of higher mass flow rates results in larger flow passages and reduced friction losses and makes it possible to use full admission conditions. The high molar mass of the working fluid implies lower values of sound speed. The few experimental data for ORC axial turbines reported in literature are compiled in Table 6. The values of turbine efficiency confirm that high-efficiency turbines (>75%) can be designed with organic fluids for the power range considered in this work. In addition to the values of Table 6, Angelino et al. [56] showed that efficiencies between 75% and 90% were obtained from ORC turbines in the electrical power range 3–500 kW. Eventually, a proper blade design with advanced techniques would enable achieving the highest possible efficiency in design and off-design conditions [57].

The results of the high-sulfur fuel case showed that the steam turbine density ratio was 149 while it was 106 for the MM turbine. These values indicate that multiple stages must be employed in the design of both turbines in order to obtain high efficiencies. In the SRC process, the formation of liquid droplets at the LP turbine outlet and the high enthalpy difference across the turbine are additional turbine design complications. The enthalpy difference across the MM turbine is 63 kJ/kg, while for the steam turbine, the enthalpy difference from the HP turbine inlet to the LP turbine outlet is 558 kJ/kg in design. The low enthalpy difference for the MM turbine indicates a design with few stages and moderate peripheral velocities. The low peripheral velocities enable a low rotational speed of the MM turbine and a direct coupling to the generator without a gearbox. This is beneficial both in terms of performance and cost and is not possible with the steam turbine. These considerations indicate that the efficiency of the MM turbine would be higher than that of the steam turbine when compared based on equal investment costs, e.g., the same number of stages.

The steam turbine in the low-sulfur fuel case was also characterized by a high density ratio (120), a high enthalpy difference (523 kJ/kg) and liquid droplet formation at the LP turbine outlet. In comparison, the values for c-pentane were significantly lower with a density ratio of 31 and an enthalpy drop of 104 kJ/kg, while the expansion was completely dry. These observations clearly indicate that higher efficiencies can be obtained for the c-pentane turbine compared to the steam turbine.

The aforementioned considerations suggest the possibility to obtain efficiency in excess of 10% points with ORC turbines compared to steam turbines, enabling higher net power production for most engine loads; see Section 3.3. This characteristic would make ORC units attractive propositions for marine waste heat recovery. In order to evaluate further the feasibility of such turbine solutions, a preliminary design study needs to be done using, for example, preliminary design tools [58].

4.2. Process Characteristics and Integration

The process layouts of the dual pressure SRC unit and the ORC unit depicted in Figures 1 and 2 indicate that the complexity of the SRC unit is higher than that of the ORC unit. The SRC unit comprises two pressure levels in the boiler, two steam drums, a turbine with dual inlets, a scavenge air cooler and multiple control valves, which are not part of the ORC unit layout. The simpler design layout of the ORC unit is favorable; however, the SRC unit layout includes the advantage of combined production of steam for service demands and steam for turbine expansion in the same boiler. The use of organic working fluids in the ORC units requires separate service steam production. In addition to this, the use of organic working fluids implies higher working fluid costs and undesirable properties like flammability, toxicity and/or global warming potential.

The once-though boiler design employed in the ORC unit enables the system to operate in sliding pressure mode for a wide range of main engine loads. To comply with the minimum boiler feed temperature, dictated by the sulfur content in the exhaust gases, it is necessary to have sufficient preheating of the working fluid at all operating conditions. As demonstrated for the high-sulfur fuel case, this is a challenge when the required boiler feed temperature is high. Only the ORC unit using the very dry fluid MM managed to reach a boiler feed temperature of 148 °C. Process layout modifications like flow extraction from the turbine for preheating and the use of scavenge air for preheating could expand the list of possible fluids for the high-sulfur fuel case. The use of scavenge air heat for preheating should be supported by other means of preheating at low engine loads where the temperature of the scavenge air drops below the required boiler feed temperature. An alternative solution could be to search for novel fluids with very dry characteristics, e.g., by use of computer-aided molecular design methods [59,60].

In the SRC unit, the scavenge air and jacket water heat are used for feed water preheating. The inclusion of the steam drums in the exhaust gas boiler layout enables a design that is less dependent on preheating than the ORC unit layout. The LP turbine throttling valve maintains the LP drum pressure at a constant value at all operating conditions, which means that the boiler feed, extracted from the bottom of the LP drum, maintains the required temperature. Therefore, it is not critical when the scavenge air temperature, and thereby the LP drum inlet temperature, drops below the required feed temperature at low loads. On the other hand, the throttling of the LP steam decreases the pressure ratio of the LP turbine and thereby also the power production. This contributes to the low performance of the SRC unit compared to the ORC units at low engine loads. An additional contribution to the throttling losses comes from the requirement of service steam production at 7 bar (165 °C). This means that the HP turbine only operates in sliding pressure mode when the HP steam pressure is above 7 bar. At low loads, the HP steam must be throttled to keep the pressure at 7 bar, resulting in lower power generation in the steam turbine.

In previous literature [61], organic fluids have been praised for their low requirement for superheating compared to steam. However, in the specific case analyzed in this paper, where a significant amount of recuperation is required in the ORC units, the degree of superheating is relatively high for most ORC solutions. The degree of superheating in terms of temperature is the highest for the SRC units, but the higher mass flow rates in the ORC units result in higher heat flow rates. The superheat is required in the ORC units in order to provide enough heat at the turbine outlet for internal recuperation. In this way, the high degree of superheating is a consequence of the high boiler feed temperature. It is usually preferable to reduce the amount of superheating, since the heat transfer performance in this part of the boiler is poor.

For both the SRC and the ORC unit, the power production is low at low main engine loads. Currently, most container ships employ slow steaming operation, meaning that most operation occurs at low engine loads. The low performance at low engine loads is a consequence of the low exhaust gas temperatures. The combined performance of the diesel engine and the WHR system can be optimized by considering the simultaneous optimization of engine tuning and WHR system design [17]. Diesel engines supplied with selective catalytic reduction (SCR) employ a special tuning enabling high temperatures at low engine loads, which is required for the operation of the SCR system [62]. This type of engine tuning could also be relevant for boosting the WHR system performance at low engine loads. The higher exhaust gas temperature comes at the cost of lower engine efficiency. This should be accounted for in the evaluation of the feasibility of alternative engine tunings.

As mentioned in Section 2.2, the size of the marine vessel is a governing factor in determining which of the ORC and SRC processes is the most feasible. For smaller ships, the service steam production takes a larger portion of the available waste heat compared to larger ships. This restricts the possible electricity production by installation of WHR units. The low power output for such an installation means that the ORC unit with a simpler process layout and turbine design is the more feasible option. If all of the exhaust gas heat is used for service steam production, WHR units can be designed to utilize the scavenge air and/or the jacket water heat. In such an integration the SRC unit is infeasible due to the combination of low temperatures and low power outputs, while the ORC unit is a relevant technology. For ships like oil tankers, heating demands can be even higher than for container ships, meaning that a large amount of service steam is required. For such ships, ORC units for harvesting low temperature sources are even more relevant.

5. Conclusions

In this paper, a design and off-design performance comparison between a state-of-the-art dual pressure SRC process and the ORC process was presented. The comparison between the processes was made based on two diesel engine waste heat recovery cases for a 4500 TEU container vessel. The engine employed a high-sulfur fuel in the first case and a low-sulfur fuel in the second case.

When the SRC and ORC processes are compared based on equal turbine efficiencies, the SRC process reaches higher net power outputs at high engine loads, while the ORC processes reach higher performance at low engine loads. The SRC process is able to reach higher performance at high engine loads, because the process layout is more advanced than the ORC layout. Contrary to the ORC process, the SRC process includes two pressure levels in the boiler, two steam drums, a turbine with dual inlets, a scavenge air cooler and multiple control valves. The ORC process enables higher performance at low engine loads due to a limited use of turbine throttling compared to the SRC process. The use of drum boilers in the SRC process requires that the pressure in the LP drum is maintained at a constant level such that the minimum temperature in the boiler does not drop below the sulfuric acid dew point. Additionally, the pressure in the HP drum must be kept at a minimum level (typically around 7 bar) in order to ensure the production of high temperature service steam. Maintaining the pressures in the steam drums requires that the steam flows to the steam turbine are throttled, which results in lower power production in the turbine. In the ORC process, the use of a dry working fluid, a once-through boiler and internal recuperation enables maintaining a high minimum temperature in the exhaust gas boiler with limited use of throttling.

Compared to the steam turbine, the ORC turbines generally expand the working fluids across a lower density (or volume) ratio and lower specific enthalpy difference without the formation of liquid droplets. Therefore, it is reasonable to expect that cost-effective turbines can be designed with higher efficiency for the ORC unit compared to the SRC unit. The results of this paper demonstrate how the turbine design efficiency value affects the off-design performance comparison between the SRC and ORC processes. For the high-sulfur fuel case, the ORC unit using MM reaches higher performance than the SRC unit at engine loads below 90%, when the turbine efficiency is 72% for the MM turbine and 62% for the steam turbine. In the low-sulfur fuel case, the ORC unit using c-pentane reaches

higher net power outputs than the SRC unit for all engine loads, when the turbine efficiencies are 72% and 62% for the c-pentane and steam turbine, respectively.

The results of this paper suggest clear performance benefits of using the ORC process compared to the SRC process. The benefits are due to the advantageous properties of the organic fluids, enabling internal heat recuperation and attractive turbine designs with high efficiencies. However, water is a beneficial working fluid considering practical aspects like fluid cost, availability and handling. For ships where all, or a major part, of the exhaust gas heat is used for service steam production, the ORC unit can be used for utilizing lower temperature sources like scavenge air and jacket water heat. This would be infeasible with an SRC unit.

Finally, it should be noted that for the low-sulfur fuel case, the SRC process produces 18% more power in design compared to the high-sulfur fuel case. For the ORC unit using MM, the increase is 33%. This indicates a high potential for WHR on ships burning low-sulfur fuels.

Acknowledgments: The work presented in this paper has been conducted within the frame of the PilotORC (www.pilotORC.mek.dtu.dk) project funded by the Danish Maritime Fond (Den Danske Maritime Fond), Project ID 2015-070; DTUMekanik, Organic Recycle Unit. The financial support is gratefully acknowledged. Furthermore, the authors would like to thank Rasmus Frimann Nielsen, Maersk, Anders Jark Jørgensen, MAN Diesel & Turbo, and Bent Ørndrup Nielsen, MAN Diesel & Turbo, for providing data for the steam Rankine cycle model validation, engine data and in general for providing useful inputs to the work.

Author Contributions: Jesper Graa Andreasen is the main author of this work. Andrea Meroni contributed with the discussion regarding turbine design and efficiency and reviewed the paper. Fredrik Haglind provided the review and guidance of the work.

Conflicts of Interest: The authors declare no conflict of interest.

Nomenclature

Symbols			*Subscripts*	
A	heat transfer area	(m^2)	0	design
C_T	Stodola constant	($K^{0.5}$/bar*kg/s)	cond	condenser
F_{CU}	copper loss fraction	()	crit	critical
h	specific enthalpy	(kJ/kg)	g	generator
$\dot{m}$	mass flow rate	(kg/s)	HP/ORC	high pressure or ORC
P	pressure	(bar)	in	inlet
T	temperature	(°C)	IP	intermediate pressure
U	overall heat transfer coefficient	(kW/K)	LP	low pressure
$\dot{V}$	volume flow rate	(m^3/s)	p	pump
$\dot{W}$	work	(kW)	out	outlet
Δ	difference	()	t	turbine
η	efficiency	(%)	sup	superheat
γ	exponent	()	sw	sea water
ρ	density	(kg/m^3)	wf	working fluid

References

1. Hou, Z.; Vlaskos, I.; Fusstetter, K.; Kahi, M.; Neuenschwander, P. New Application Fields for Marine Waste Heat Systems by Analysing the Main Design Parameters. In Proceedings of the CIMAC Congress, Vienna, Austria, 21–24 May 2007.
2. MAN Diesel & Turbo. *Waste Heat Recovery System (WHRS) for Reduction of Fuel Consumption, Emission and EEDI*; Technical Report; MAN Diesel & Turbo: Augsburg, Germany, 2012.
3. Ma, Z.; Yang, D.; Guo, Q. Conceptual Design and Performance Analysis of an Exhaust Gas Waste Heat Recovery System for a 10000TEU Container Ship. *Pol. Marit. Res.* **2012**, *19*, 31–38.
4. Benvenuto, G.; Trucco, A.; Campora, U. Optimization of waste heat recovery from the exhaust gas of marine diesel engines. *Proc. Inst. Mech. Eng. Part M J. Eng. Marit. Environ.* **2016**, *230*, 83–94.
5. Dimopoulos, G.G.; Georgopoulou, C.A.; Kakalis, N.M.P. Modelling and optimization of an integrated marine combined cycle system. In Proceedings of the ECOS, Novi Sad, Serbia, 4–7 July 2011; pp. 1283–1298.

6. Theotokatos, G.; Livanos, G.A. Modern Concepts of Ferries Propulsion Plant for Reducing Fuel Consumption Cost and CO 2 Emissions. In Proceedings of the Low Carbon Shipping Conference, London, UK, 9–10 September 2013; pp. 1–12.
7. Öhman, H.; Lundqvist, P. Comparison and analysis of performance using Low Temperature Power Cycles. *Appl. Therm. Eng.* **2013**, *52*, 160–169.
8. Yuksek, E.L.; Mirmobin, P. Waste heat utilization of main propulsion engine jacket water in marine application. ASME ORC 2015. In Proceedings of the 3rd International Seminar on ORC Power Systems, Brussels, Belgium, 12–14 October 2015; pp. 1–10, Paper ID: 42.
9. Larsen, U.; Pierobon, L.; Haglind, F.; Gabrielii, C. Design and optimisation of organic Rankine cycles for waste heat recovery in marine applications using the principles of natural selection. *Energy* **2013**, *55*, 803–812.
10. Yang, M.H.; Yeh, R.H. Analyzing the optimization of an organic Rankine cycle system for recovering waste heat from a large marine engine containing a cooling water system. *Energy Convers. Manag.* **2014**, *88*, 999–1010.
11. Yang, M.H.; Yeh, R.H. Thermodynamic and economic performances optimization of an organic Rankine cycle system utilizing exhaust gas of a large marine diesel engine. *Appl. Energy* **2015**, *149*, 1–12.
12. Kalikatzarakis, M.; Frangopoulos, C.A. Multi-criteria selection and thermo-economic optimization of Organic Rankine Cycle system for a marine application. In Proceedings of the ECOS, Turku, Finland, 15–19 June 2014; pp. 1–15.
13. Choi, B.C.; Kim, Y.M. Thermodynamic analysis of a dual loop heat recovery system with trilateral cycle applied to exhaust gases of internal combustion engine for propulsion of the 6800 TEU container ship. *Energy* **2013**, *58*, 404–416.
14. Yun, E.; Park, H.; Yoon, S.Y.; Kim, K.C. Dual parallel organic Rankine cycle (ORC) system for high efficiency waste heat recovery in marine application. *J. Mech. Sci. Technol.* **2015**, *29*, 2509–2515.
15. Soffiato, M.; Frangopoulos, C.A.; Manente, G.; Rech, S.; Lazzaretto, A. Design optimization of ORC systems for waste heat recovery on board a LNG carrier. *Energy Convers. Manag.* **2015**, *92*, 523–534.
16. Baldi, F.; Larsen, U.; Gabrielii, C. Comparison of different procedures for the optimisation of a combined Diesel engine and organic Rankine cycle system based on ship operational profile. *Ocean Eng.* **2015**, *110*, 85–93.
17. Larsen, U.; Pierobon, L.; Baldi, F.; Haglind, F.; Ivarsson, A. Development of a model for the prediction of the fuel consumption and nitrogen oxides emission trade-off for large ships. *Energy* **2015**, *80*, 545–555.
18. Ahlgren, F.; Mondejar, M.E.; Genrup, M.; Thern, M. Waste Heat Recovery in a Cruise Vessel in the Baltic Sea by Using an Organic Rankine Cycle: A Case Study. *J. Eng. Gas Turbines Power* **2015**, *138*, 011702.
19. Mondejar, M.E.; Ahlgren, F.; Thern, M.; Genrup, M. Quasi-steady state simulation of an organic Rankine cycle for waste heat recovery in a passenger vessel. *Appl. Energy* **2015**, pp. 1–12.
20. Larsen, U.; Sigthorsson, O.; Haglind, F. A comparison of advanced heat recovery power cycles in a combined cycle for large ships. *Energy* **2014**, *74*, 260–268.
21. Suárez de la Fuente, S.; Greig, A. Making shipping greener: Comparative study between organic fluids and water for Rankine cycle waste heat recovery. *J. Mar. Eng. Technol.* **2015**, *14*, 70–84.
22. Suárez de la Fuente, S.; Roberge, D.; Greig, A.R. Safety and CO2 emissions: Implications of using organic fluids in a ship's waste heat recovery system. *Mar. Policy* **2016**, pp. 1–13.
23. Yang, D.; Zheshu, M. Conceptual design and performance analysis of waste heat recovery system for intelligent marine diesel engines. Part 1: Impractical analysis of traditional WHR systems. *Heat Technol.* **2012**, *30*, 85–92.
24. Grljušić, M.; Medica, V.; Račić, N. Thermodynamic analysis of a ship power plant operating with waste heat recovery through combined heat and power production. *Energies* **2014**, *7*, 7368–7394.
25. Quoilin, S.; van den Broek, M.; Declaye, S.; Dewallef, P.; Lemort, V. Techno-economic survey of Organic Rankine Cycle (ORC) systems. *Renew. Sustain. Energy Rev.* **2013**, *22*, 168–186.
26. Official Journal of the European Union. *Regulation (EU) No 517/2014 of the European Parliament and of the Council on Fluorinated Greenhouse Gases and Repealing Regulation (EC) no 842/2006*; Technical Report; European Union: Brussels, Belgium, 2014.
27. UN Environment. The Kigali Amendment to the Montreal Protocol: Another Global Commitment to Stop Climate Change. 2016. Available online: web.unep.org/kigali-amendment-montreal-protocol-another-global-commitment-stop-climate-change (accessed on 15 February 2017).

28. Solvay. Solkatherm Datasheet. 2016. Available online: www.solvay.com/en/markets-and-products/featured-products/SOLKATHERM-SES36.html (accessed on 15 February 2017).
29. Invernizzi, C.; Bonalumi, D. Thermal stability of organic fluids for Organic Rankine Cycle systems. In *Organic Rankine Cycle (ORC) Power Systems*; Macchi, E., Astolfi, M., Eds.; Woodhead Publishing: Amsterdam, The Netherlands, 2017; pp. 121–151.
30. Colonna, P.; Casati, E.; Trapp, C.; Mathijssen, T.; Larjola, J.; Turunen-Saaresti, T.; Uusitalo, A. Organic Rankine Cycle Power Systems: From the Concept to Current Technology, Applications, and an Outlook to the Future. *J. Eng. Gas Turbines Power* **2015**, *137*, 100801.
31. MAN Diesel & Turbo. CEAS Engine Calculation Tool. Available online: marine.man.eu/two-stroke/ceas (accessed on 15 February 2017).
32. Bell, I.H.; Wronski, J.; Quoilin, S.; Lemort, V. Pure and Pseudo-pure Fluid Thermophysical Property Evaluation and the Open-Source Thermophysical Property Library CoolProp. *Ind. Eng. Chem. Res.* **2014**, *53*, 2498–2508.
33. International Maritime Organization. *Sulfur Oxides (SOx) Regulation 14*; Technical Report; International Maritime Organization: London, UK, 2015.
34. MAN Diesel & Turbo. *Soot Deposits and Fires in Exhaust Gas Boilers*; Technical Report; MAN Diesel & Turbo: Copenhagen, Denmark, 2014.
35. Pierobon, L.; Benato, A.; Scolari, E.; Haglind, F.; Stoppato, A. Waste heat recovery technologies for offshore platforms. *Appl. Energy* **2014**, *136*, 228–241.
36. Grimson, E. Correlation and utilization of new data on flow resistance and heat transfer for cross flow of gases over tube banks. *Trans. Am. Soc. Mech. Eng.* **1937**, *59*, 583–594.
37. Holman, J.P. *Heat Transfer*; McGraw-Hill Companies: Singapore, 2010.
38. Dittus, W.; Boelter, L.M.K. Heat transfer in automobile radiators of the tubular type. *Int. Commun. Heat Mass Transf.* **1930**, *2*, 443–461.
39. Lecompte, S.; Huisseune, H.; van den Broek, M.; De Schampheleire, S.; De Paepe, M. Part load based thermo-economic optimization of the Organic Rankine Cycle (ORC) applied to a combined heat and power (CHP) system. *Appl. Energy* **2013**, *111*, 871–881.
40. Veres, J. *Centrifugal and Axial Pump Design and Off-Design Performance Prediction*; Technical Report; NASA: Sunnyvale, CA, USA, 1994.
41. Erhart, T.; Eicker, U.; Infield, D. Part-load characteristics of Organic-Rankine-Cycles. In Proceedings of the 2nd European Conference on Polygeneration, Tarragona, Spain, 30 March–1 April 2011; pp. 1–11.
42. Stodola, A. *Dampf- und Gasturbinen: Mit einem Anhang über die Aussichten der Wärmekraftmaschinen*; Springer: Berlin, Germany, 1922.
43. Haglind, F.; Elmegaard, B. Methodologies for predicting the part-load performance of aero-derivative gas turbines. *Energy* **2009**, *34*, 1484–92.
44. Macchi, E. Design criteria for turbines operating with fluids having a low speed of sound. In *Von Karman Institute For Fluid Dynamics, Lecture Series 100*; Von Karman Institute For Fluid Dynamics: Rhode-Saint-Genése, Belgium, 1977.
45. Macchi, E. Theoretical basis of the Organic Rankine Cycle. In *Organic Rankine Cycle (ORC) Power Systems*; Woodhead Publishing: Amsterdam, The Netherlands, 2017; pp. 3–24.
46. Owen, J.R. *The Organic Rankine Cycle: A Review of Applications and Factors Affecting Working Fluid Selection*; City University: London, UK, 1975.
47. Angelino, G.; Gaia, M.; Macchi, E. Medium temperature 100 kW ORC engine for total energy systems. In *Energy Conservation in Industry—Combustion, Heat Recovery and Rankine Cycle Machines*; Ehringer, H., Hoyaux, G., Pilavachi, P.A., Eds.; Springer Science: Dordrecht, The Netherlands, 1983; pp. 177–189.
48. Kraus, M.H.; Deichsel, M.; Hirsch, P.; Opferkuch, F.; Heckel, C. Hermetic 40-kW-Class Steam Turbine System for the Bottoming Cycle of Internal Combustion Engines. In Proceedings of the ASME Turbo Expo 2016: Turbomachinery Technical Conference and Exposition, Seoul, Korea, 13–17 June 2016; pp. 1–10.
49. Verdonk, G.; Dufournet, T. Development of a supersonic steam turbine with a single stage pressure ratio of 200 for generator and mechanical drive. In *Von Karman Institute for Fluid Dynamics, Small High Pressure Ratio Turbines*; Von Karman Institute For Fluid Dynamics: Rhode-Saint-Genése, Belgium, 1987.
50. Bahadori, A.; Vuthaluru, H.B. Estimation of performance of steam turbines using a simple predictive tool. *Appl. Therm. Eng.* **2010**, *30*, 1832–1838.

51. Darrow, K.; Tidball, R.; Wang, J.; Hampson, A. *Section 4. Technology Characterization—Steam Turbines*; Technical Report; U.S. Environmental Protection Agency Combined Heat and Power Partnership: Washington, DC, USA, 2015.
52. Elliott Group. Steam Turbine Calculator. Available online: www.elliott-turbo.com/TurbineCalculator (accessed on 15 February 2017).
53. Angelino, G.; Bini, R.; Bombarda, P.; Gaia, M.; Girardi, P.; Lucchi, P.; Macchi, E.; Rognoni, M.; Sabatelli, F. One MW binary cycle turbogenerator module made in Europe. In Proceedings of the World Geothermal Congress, Firenze, Italy, 18–31 May 1995; Volume 3, pp. 2125–2130.
54. Verneau, A. Supersonic turbines for organic fluid Rankine cycles from 3 to 1300 kW. In *Von Karman Institute for Fluid Dynamics, Small High Pressure Ratio Turbines*; Von Karman Institute For Fluid Dynamics: Rhode-Saint-Genése, Belgium, 1987.
55. Klonowicz, P.; Borsukiewicz-Gozdur, A.; Hanausek, P.; Kryłłowicz, W.; Brüggemann, D. Design and performance measurements of an organic vapor turbine. *Appl. Therm. Eng.* **2014**, *63*, 297–303.
56. Angelino, G.; Gaia, M.; Macchi, E. A review of Italian activity in the field of organic Rankine cycles. *VDI-Berichte* **1984**, *539*, 465–482.
57. Persico, G.; Pini, M. Fluid dynamic design of Organic Rankine Cycle turbines. In *Organic Rankine Cycle (ORC) Power Systems*; Woodhead Publishing: Amsterdam, The Netherlands, 2017; pp. 253–297.
58. Meroni, A.; La Seta, A.; Andreasen, J.; Pierobon, L.; Persico, G.; Haglind, F. Combined Turbine and Cycle Optimization for Organic Rankine Cycle Power Systems—Part A: Turbine Model. *Energies* **2016**, *9*, 313.
59. Papadopoulos, A.I.; Stijepovic, M.; Linke, P. On the systematic design and selection of optimal working fluids for Organic Rankine Cycles. *Appl. Therm. Eng.* **2010**, *30*, 760–769.
60. Zhang, L.; Cignitti, S.; Gani, R. Generic mathematical programming formulation and solution for computer-aided molecular design. *Comput. Chem. Eng.* **2015**, *78*, 79–84.
61. Chen, H.; Goswami, D.Y.; Stefanakos, E.K. A review of thermodynamic cycles and working fluids for the conversion of low-grade heat. *Renew. Sustain. Energy Rev.* **2010**, *14*, 3059–3067.
62. MAN Diesel & Turbo. *Emission Project Guide*; Technical Report; MAN Diesel & Turbo: Copenhagen, Denmark, 2016.